UWB Radio Propagation Measurements in a Desktop Environment

Duje Čoko, Dinko Begušić, and Zoran Blažević

Original scientific paper

Abstract: **The ultra-wideband wireless personal area networks are expected to be most commonly employed in desktop environments. This paper presents a measurement campaign conducted on a typical office desk. A pair of omnidirectional UWB antennas and a vector network analyzer were used to measure the impulse responses over a frequency range spanning from 6 GHz to 8.5 GHz, in accordance with the UWB regulations in Europe. The coherence bandwidth and the rms delay spread are calculated from the measurement results. A significant correlation between these wideband parameters is found, but only at higher correlation thresholds.**

Index terms: **ultra-wideband, desktop propagation, delay spread, coherence bandwidth**

I. Introduction

Ultra-wideband (UWB) technology is a promising candidate for short range, high data rate systems. FCC regulations in the USA authorize the unlicensed use of UWB in the range from 3.1 to 10.6 GHz [1]. The power spectral density emission limit for UWB emitters operating in the UWB band is -41.3 dBm/MHz. This is the same limit that applies to unintentional emitters in the UWB band, known as Part 15 limit. In Europe, the ECC decision is more restrictive, narrowing the range from 6 to 8.5 GHz [2].

This paper deals with UWB signal propagation on an empty desktop surface located in a furnished office room. The measurements were taken in accordance to the ECC regulations. A similar measurement campaign may be found in [3]. Over the past few years the UWB systems have been researched extensively, resulting in numerous published papers, covering a wide range of topics, such as signal propagation [4,5], channel modeling [6,7,8], interference analysis [9], etc. Most of these studies are carried out in the FCC frequency range. The wireless signal propagation in desktop environments has also been studied at higher frequencies, in millimeter wave region [10] and at 60 GHz [11,12].

Manuscript received June 30, 2009; revised June 11, 2010**.** The material in this paper was presented in part at the 17th International Conference on Software, Telecommunications and Computer Networks (SoftCOM 2009), Split-Hvar-Korčula, Croatia, Sept. 2009.

Authors are with the Department of electronics, FESB, University of Split, Croatia (e-mail: {dcoko, begusic, zblaz}@fesb.hr).

Along with an extensive set of channel measurements in the ECC frequency range, the novelties in this paper include an analysis of correlation between the measured delay spread and coherence bandwidth, resulting in a conclusion that a certain correlation exists only at a higher correlation threshold. In such specific LOS scenario the coherence bandwidth should not be estimated directly from the measured delay spread.

In the next section the measurement system and procedure will be explained. The third section presents the measurement results, while the fourth section deals with the channel parameters derived from the measured data, which describe the time dispersive nature of the channel.

II. Measurement procedure

The measurements were conducted on a surface of a typical office desk made of chipboard, placed in one of the office rooms in our university building, as presented on Fig. 1. The desktop surface was cleared in order to insure the line-of-sight (LOS) radio path between the transmitting and the receiving antenna.

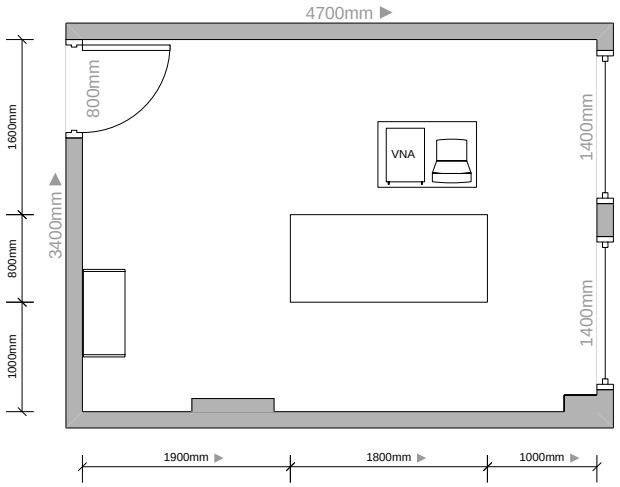

Fig. 1. Office plan

Inner walls that separate offices and laboratories are mainly made of plasterboard constructed with a thin wire grid composition while the external wall and floors are made of

reinforced concrete. The floor is entirely covered with wooden parquetry; the doors are made of plywood, while the office furniture is made of various wooden materials.

A 1600x700 mm grid with 100 mm step, placed on the desk. The *x* axis was parallel to the longer desk edge, while the *y* edge was placed at the centerline. As the measurements were conducted, the transmitting antenna was located at the grid origin, 50 mm from the back side of the desk, while the receiving antenna was moved along the remaining 135 points on the grid for each measurement.

The measurement system consists of a HP 8720A vector network analyzer, two omnidirectional antennas, a semi rigid coaxial cable and a flexible coaxial cable. The antennas are built according to the two-circular-hole planar inverted cone model [13], etched on a printed circuit board and mounted on a copper disc ground plane. Both antennas have a reasonably flat frequency response, and VSWR less than 1.5 throughout the entire frequency range from 6 to 8.5 GHz, as shown in Fig. 2. The antennas were raised 75 mm above the desk to make space for cable connections. As the measurements were taken, a special attention was paid to proper antenna placement, as well as leveling the ground planes to avoid any gain or loss caused by the elevation pattern.

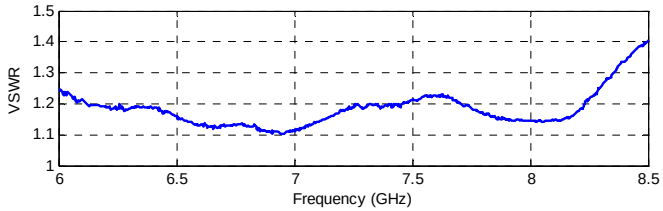

Fig. 2. Measured VSWR

In accordance to the ECC spectral mask, Fig. 3, the VNA output power level was set to -10 dBm, resulting in a power spectral density lower than -41.3 dBm/MHz. The frequency range of the measurements was 6 – 8.5 GHz, with 801 frequency points per sweep.

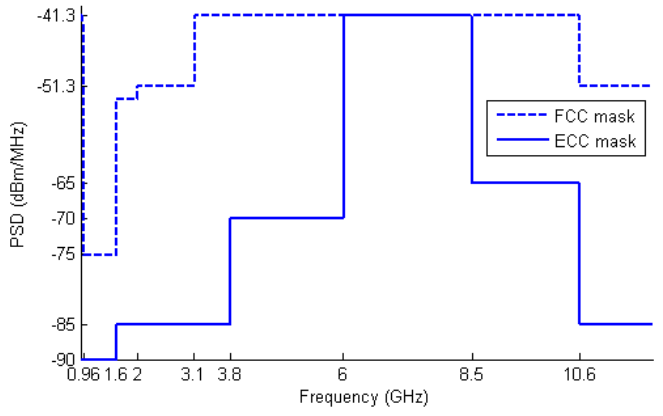

Fig. 3. FCC and ECC spectrum mask for indoor UWB

The inverse Fourier Transform was used to convert the frequency domain data to corresponding time domain responses. In order to extend the measurement system dynamic range, following the frequency response calibration, an averaging function was enabled. This resulted in reduction of the random noise effect and time-variability of the channel, as each measurement result is averaged by sets of 16 successive sweeps. The measurement setup is presented on Fig. 4.

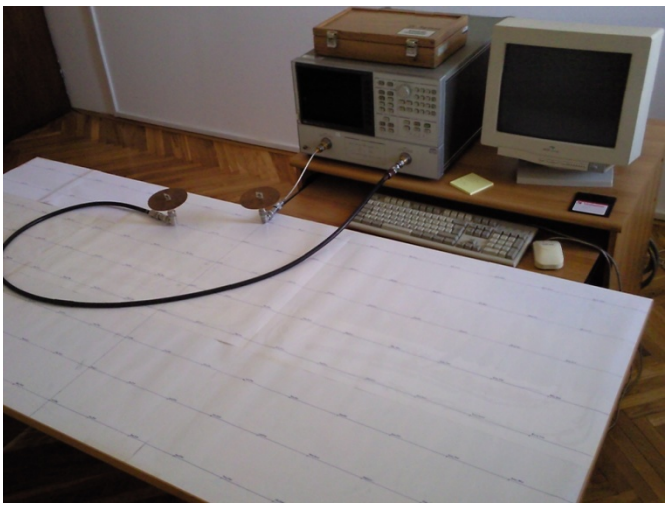

Fig. 4. Measurement setup

III. MEASURED IMPULSE RESPONSES

Once properly calibrated, the VNA measures the band-limited frequency transfer function **H** of the channel as:

$$\mathbf{H}_{meas}(f) = W(f)\mathbf{H}(f) \tag{1}$$

and converts the results to the time domain by utilizing the time domain capability as:

$$\mathbf{h}_{meas}(t) = w(t) \otimes \mathbf{h}(t) = \Im^{-1}\{W(f)\mathbf{H}(f)\}, \tag{2}$$

where

$$w(t) = \Im^{-1}\{W(f)\}, \tag{3}$$

is the inverse Fourier Transform $\Im^{-1}$ of the frequency window $W(f)$ used by VNA, determined by measurement bandwidth, and:

$$\mathbf{h}(t) = \Im^{-1}\{\mathbf{H}(f)\}, \tag{4}$$

is the channel impulse response.

Using the inverse Fourier Transform the impulse response is obtained from the measured frequency response, giving the power delay profile as $P_h(t) = |h_{meas}(t)|^2$, where $h_{meas}(t)$ is a band-limited measured version of $h(t)$ [14].

Two examples of measured power delay profiles at points (0,200) and (800,700) are presented on Fig. 5 and Fig. 6, respectively.

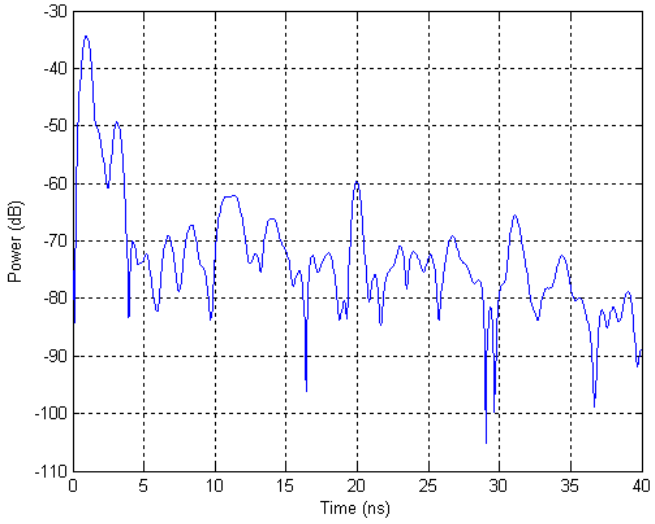

Fig. 5. Power delay profile at 0,200

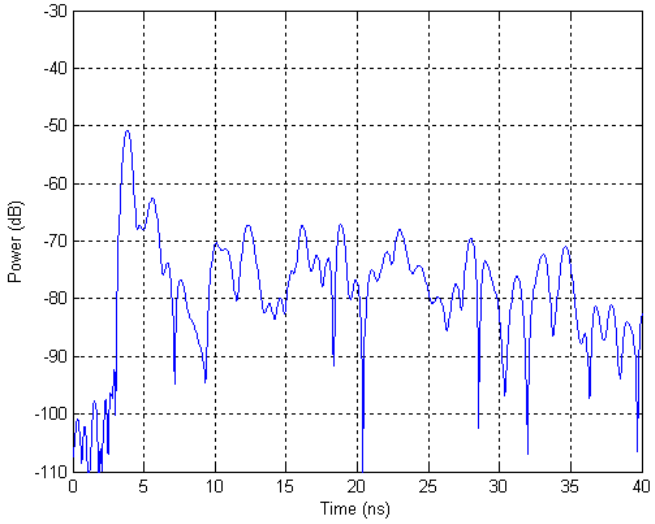

Fig. 6. Power delay profile at 800,700

As there were no obstructions of the LOS radio path during the measurement procedure, these power delay profiles are characterized by the dominant first ray in the first cluster. Comparing the two presented profiles it is evident that as the path length increases, the first ray amplitude gets impaired and the time of first ray arrival gets longer. As these two parameters are hard to compare on a large number of measured profiles, they will be presented in form of contour plots, where *x* and *y* axes are equal to the desktop grid.

In these measurements the first ray is always the direct ray, which attenuation is determined by the free space path loss. The first ray amplitude for each measurement point is presented on Fig. 7. Some minor discrepancies are present, most likely due to the presence of the measurement equipment. Fig. 8 presents the first ray arrival time contour plot obtained from the measurement results. It can be seen that the values are evenly distributed in shape of concentric half circles. This is expected, since the first ray arrival time is directly proportional to the antenna separation.

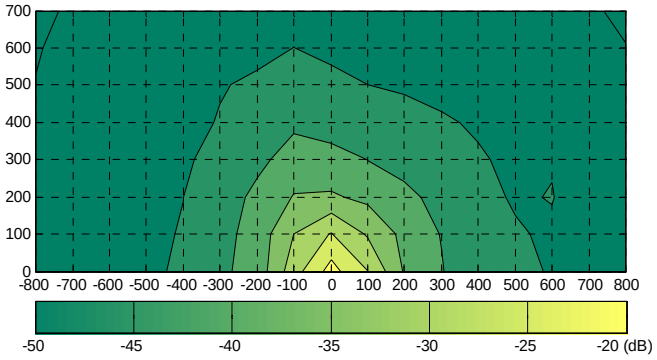

Fig. 7. First ray amplitude

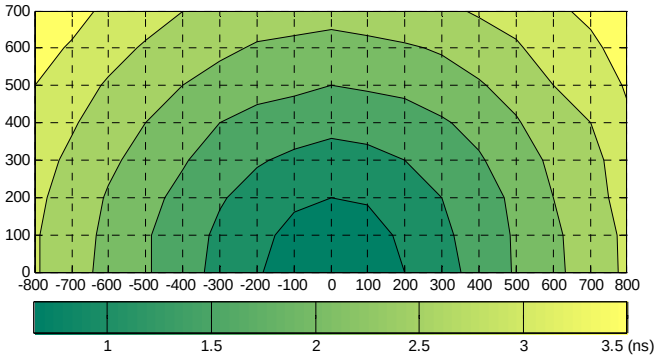

Fig. 8. First ray arrival time

IV. Delay Spread and Coherence Bandwidth

The rms delay spread provides a raw estimation of the channel while the coherence bandwidth B_c at some correlation threshold $C \in (0, 1)$ defines the measure of frequency selectivity of the wideband channel. Both parameters can be calculated directly from the measured frequency averaged power delay profile [15]. The n^{th} moment of the received power delay profiles is given by:

$$m_n = \int_{-\infty}^{+\infty} t^n P_h(t)\, dt, \tag{5}$$

and the rms delay spread can be calculated as:

$$\sigma_t = \sqrt{\frac{m_2}{m_0} - \left(\frac{m_1}{m_0}\right)^2}. \tag{6}$$

Applying the Fourier Transform on measured power delay profile, we obtain the maximum frequency separation Δf, or the coherence bandwidth B_c, over which the channel can be considered flat:

$$R_h(\Delta f) = \Im\{P_h(t)\} \rightarrow |R_h(\Delta f = B_C)| = C \qquad (7)$$

where C represents the correlation threshold [15].

As for the connection to the delay-spread, an inverse proportionality of these channel parameters has been observed in numerous references. Moreover, the theoretical minimum coherence bandwidth $B_{C\min}$ is derived under the assumption of a wide-sense stationary channel in [16] as:

$$B_{C\min} = \frac{\arccos C}{2\pi\sigma_t} \qquad (8)$$

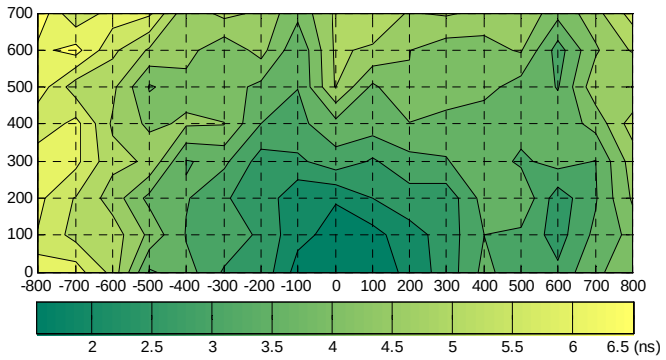

Fig. 9. RMS delay spread estimation

The rms delay spread is calculated for each measurement point using the expressions (5, 6). The results are presented in form of a contour plot on Fig. 9. As expected, the rms delay spread increases as the radio path gets longer, although some discrepancies exist in certain regions of the desktop surface, due to the multipath propagation caused by the reflections in the room, at measurement equipment, and on the desk itself, such as two local minima at $x = 600$.

The coherence bandwidth is calculated from the measured data according to (7) for two commonly used correlation thresholds, $C_1 = 0.9$, Fig. 10 and $C_2 = 0.707$, Fig. 11. The results show that a higher threshold yields a more narrow coherence bandwidth. The minimum coherence bandwidth estimated from the measured delay spread (8) exhibits much lower values than those calculated from (7) for both correlation thresholds. This is caused by multiple reflections on the desktop surface which increase the delay spread while not affecting the coherence bandwidth to same extent.

TABLE I

CORRELATION ρ BETWEEN THE MEASURED RMS DELAY SPREAD AND COHERENCE BANDWIDTH AT DIFFERENT THRESHOLDS C

C	0.9	0.707
ρ	-0.76	-0.24

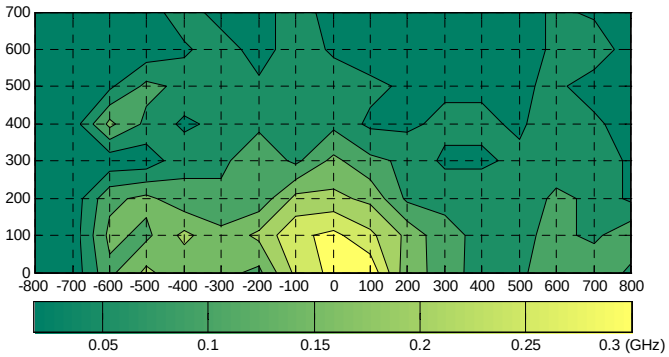

Fig. 10. Estimated coherence bandwidth at correlation threshold C_1

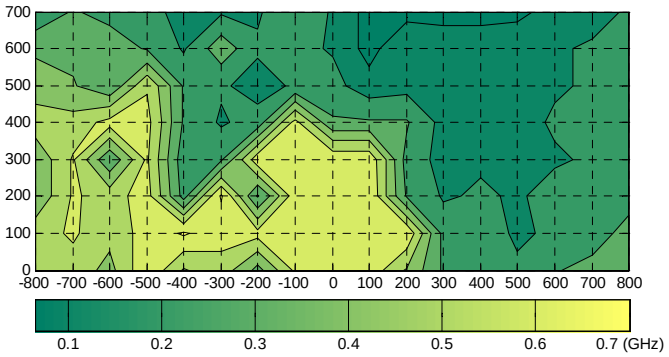

Fig. 11. Estimated coherence bandwidth at correlation threshold C_2

Comparing the rms delay spread plot with two different coherence bandwidth plots it can be noticed that a higher correlation threshold yields a certain correlation between these two parameters, while the lower threshold results in very low correlation. Correlation coefficients between the measured rms delay spread and coherence bandwidth are calculated for each threshold and presented in Table 1. The negative values show that the delay spread and coherence bandwidth are inversely proportional.

V. CONCLUSION

This paper presented an UWB channel measurement campaign carried out on an office desk. A pair of UWB omnidirectional antennas was built and used with a vector network analyzer to measure the impulse responses at evenly distributed points on an empty desktop surface.

The rms delay spread and coherence bandwidth were estimated from the measured data in order to find a correlation between them. The coherence bandwidth was calculated for two different correlation thresholds. From the graphical presentation of the results it was evident that there was no significant delay spread – coherence bandwidth correlation for the lower correlation threshold, while the higher threshold level exhibited a noticeable amount of correlation. The corresponding correlation coefficients were calculated to confirm this observation.

Multiple reflections on the desktop surface increase the delay spread while not affecting the coherence bandwidth in same amount. For this reason, the coherence bandwidth should not be estimated directly from the rms delay spread when designing an UWB communication channel in similar environments.

REFERENCES

[1] FCC First Report and Order 02-48, "In the matter of Revision of Part 15 of the Commission's Rules Regarding Ultra-Wideband Transmission Systems", April 2002.

[2] ECC Decision (06)04, "On the harmonized conditions for devices using Ultra-Wideband (UWB) technology in bands below 10.6 GHz", July 2007.

[3] Y. Suzuki, T. Kobayashi: *Ultra Wideband Signal Propagation in Desktop Environments*, in Proc. of IEEE Conference on Ultra Wideband Systems and Technologies, Vol. 16, No. 19, pp. 493-497, November 2003.

[4] Y.W. Yeap, O.M. Chi, C.L. Law: *Evaluation of Ultra Wideband (UWB) Signal Transmission*, Propagation and Reception with Low Cost UWB RF Front End", in Proc. of IEEE International RF and Microwave Conference 2004, pp. 72-75, October 2004.

[5] A.H. Muqaibel et al.: *Measurement and Characterization of Indoor Ultra-Wideband Propagation*, in Proc. of IEEE Conference on Ultra Wideband Systems and Technologies, pp. 295-299, November 2003.

[6] Z. Irahhauten, H. Nikookar, G.J.M. Janssen: *An Overview of Ultra Wide Band Indoor Channel Measurements and Modeling*, IEEE Microwave and Wireless Components Letters, Vol.14, No.8, pp. 386-388, August 2004.

[7] N. Xin, D.G. Michelson: *Frequency Domain Analysis of the IEEE 802.15.4a Standard Channel Models*, in Proc. of IEEE Wireless Communications and Networking Conference 2007, pp. 2058-2062, March 2007.

[8] A. Fort et al.: *Ultra-Wideband Channel Model for Communication Around the Human Body*, IEEE Journal on Selected Areas in Communications, Vol.24, No.4, pp. 927-933, April 2006.

[9] Y. Chen, N.C. Beaulieu: *Interference Analysis of UWB Systems for IEEE Channel Models Using First- and Second-Order Moments*, IEEE Transactions on Communications, Vol.57, No.3, pp. 622-625, March 2009.

[10] N. Kuribayashi, W. Yue: *Studies on Millimeter Wave 3 Gbps Wireless Access Systems*, IEEE International Workshop on Broadband Convergence Networks 2007, pp. 1-5, May 2007.

[11] C. Liu, E. Skafidas, R.J. Evans: *Characterization of the 60 GHz Wireless Desktop Channel*, IEEE Transactions on Antennas and Propagation, Vol.55, No.7, pp. 2129-2133, July 2007.

[12] A.F. dos Santos, W. Rave, G. Fettweis: *Iterative blind receiver exploiting channel code constraints for 60 GHz UWB channels*, in Proc. of IEEE International Conference on Ultra-Wideband, Vol.2, pp. 41-44, September 2008.

[13] S.-Y. Suh, W. L. Stutzman, W.A. Davis: *A New Ultra wideband Printed Monopole Antenna: The Planar Inverted Cone Antenna (PICA)*, IEEE Transactions on Antennas and Propagation, Vol.52, No.5, pp. 1361-1365, May 2004.

[14] Z. Blažević, I. Zanchi, I. Marinović: *Wideband Measurements and Analysis of the Single-Floor Indoor Radio Channel at 2.4 GHz*, in Proc. of the International Conference on Applied Electromagnetics and Communications ICECom '07, pp. 347-351, October 2007.

[15] Z. Blažević, I. Zanchi, I. Marinović: *Propagation Measurements at 2.4 GHz Inside a University Building and Estimation of Saleh-Valenzuela Parameters*, Journal of Communications Software and Systems, Vol.3, No.2, pp. 99-107, 2007.

[16] H. Fleury: *An Uncertainty Relation for WSS Processes and Its Applications to WSSUS Systems*, IEEE Transactions on Communications, Vol.44, No.12, pp. 1632-1634, December 1996.

Duje Čoko was born in Split, Croatia, in 1983. He received the B.S. degree in 2007 at University of Split, Faculty of Electrical Engineering, Mechanical Engineering and Naval Architecture (FESB), Split, Croatia.
He is presently a Research Assistant at the Dept. of Electronics, FESB. His fields of interest include electronic circuits and ultra wideband radio propagation.
He is a member of IEEE from 2007.

Dinko Begušić received the B.S. degree in electrical engineering from the University of Split, Croatia in 1983, and the M.S. and Ph.D degrees in electrical engineering from the University of Zagreb, Croatia, in 1988 and 1992, respectively.
Since 1985, he has been with the University of Split, Croatia. He is a professor and the chair of the communication technologies and signal processing at the Faculty of Electrical Engineering, Mechanical Engineering and Naval Architecture (FESB). From September 1990 to June 1991, he was a visiting researcher with the Universite Libre de Bruxelles, Bruxelles, Belgium. From February through July 1992, he was visiting researcher with the King's College London, London, UK. From September 1997 until May 1998, he was with the University of Texas at Dallas, Richardson, TX, as a Visiting Assistant Professor. His research interests include communication systems and networks, digital signal processing for communications and adaptive algorithms.
Dr. Begušić is a Co-Chair of the Conference on Software, Telecommunications and Computer Networks SoftCOM.

Zoran Blažević was born in Split, Croatia in 1968. He received his B.S. degree 1993, M.S. degree 2000 and Ph.D. 2005 at University of Split, Faculty of Electrical Engineering, Mechanical Engineering and Naval Architecture (FESB), Split, Croatia.
From 1994-1996 he was with Croatian Railways working as a telecommunication engineer, and from 2001-2006 was a research assistant at the Dept. of Electronics, FESB. Since 2006 he is an Assistant Professor at the same university engaged in projects tied with radio-communications.
Dr. Blažević is a member of IEEE from 2006.